

Designing and Simulating High Enthalpy Expansion Tube Conditions

By Chris James¹⁾, David E. Gildfind¹⁾, Richard G. Morgan¹⁾, Peter A. Jacobs²⁾, and Fabian Zander¹⁾

¹⁾The Centre for Hypersonics, The University of Queensland, Brisbane, Australia

²⁾Queensland Geothermal Energy Centre of Excellence, The University of Queensland, Brisbane, Australia

This paper details a new expansion tube parametric analysis code, PITOT. This new code aims to provide a user-friendly, flexible, and specialised expansion tube analysis tool, which can be used to rapidly design new expansion tube flow conditions, and also rapidly characterise actual experimental test flows. The paper begins by providing an overview of expansion tube wind tunnel facilities, and details The University of Queensland's X2 and X3 facilities. It then describes the new PITOT code, including its functionality, intended application, and underlying theoretical framework. Some benefits of this code compared to previous analytical routines are its user-friendly interface, and its robust implementation of equilibrium gas principles, including its library of different test gases. The paper presents preliminary results comparing PITOT predictions with CFD and experimental results, generally showing good agreement, and demonstrating the value of having an improved, short run time, flow condition design tool.

Key Words: Expansion Tube, Hypersonics, Ground Testing, Facility Configuration, CFD

1. Introduction

Expansion tubes are the only wind tunnels able to recreate the flight of vehicles entering the atmospheres of distant planets, at speeds between 6 and 15 km/s. And recently, for the first time, The University of Queensland (UQ) generated the high energy flows which a scramjet-powered launch vehicle will endure before leaving Earth's atmosphere¹⁾. Expansion tubes are not constrained by the total pressure and temperature limitations of other impulse facilities which stagnate their test gas, such as reflected shock tunnels (RSTs). While test times are short in expansion tubes (10's to 100's of μ s), these facilities provide a unique capability which is becoming increasingly necessary to support continuing advances in hypersonics research into the 21st century.

As will be explained later in this paper, the expansion tube relies on the careful control of many complex flow processes, and configuration of these machines, and characterisation of their test flows, is not a trivial exercise. The University of Queensland (UQ) has extensive experience with the development and operation of the *free-piston driven* expansion tube, which, as its name suggests, has the additional complexity of a free-piston (as opposed to the simpler fixed volume) driver. This is the most powerful variation of the expansion tube concept, and in X3, UQ has the world's most powerful free-piston driven expansion tube. This paper first discusses the expansion tube concept, it details UQ's two currently operation expansion tubes – the X2 and recently upgraded X3 facilities – and then discusses the development of a new code, PITOT, to assist in the development and characterization of new flow conditions in these sophisticated hypersonic wind tunnels.

2. Principle of Operation

Resler and Bloxom²⁾ originally proposed the expansion tube concept in 1952, which is essentially a modification to the shock tube concept. Trimpi^{3,4)} later derived the analytical tools which are still used to this day to make approximate predictions of their performance. Fig. 1 shows a schematic diagram of the configuration of an expansion tube, and also the wave processes which are generated during its operation. The facility comprises three primary structural components/assemblies, as follows:

1. Free-piston driver (the left side of Fig. 1): A heavy piston is initially held in position, inside a large diameter steel 'compression tube', which is sealed from the downstream tube by a strong steel diaphragm. A light gas (such as helium), at relatively low pressure (~ 1 atm) initially fills the volume between the piston front face and the steel diaphragm. Behind the piston is a large volume of high pressure air (~ 10 - 100 's atm).
2. Driven tube (centre of Fig. 1): downstream of the steel diaphragm is a long steel tube. This tube can be opened at various junctures along its length, and thin diaphragms (typically Mylar) are then used to divide this tube into sealed compartments of various lengths. Referring to Fig. 1, UQ sometimes operates these facilities by filling the first section with helium (~ 1 atm), and this tube is referred to as the 'secondary driver'; the function of this tube is discussed later. Next is the test gas (~ 10 's kPa for superorbital flight speeds, or 100 's kPa for scramjet flight conditions); this section of tube is referred to as the 'shock tube'. The remainder of the tube, downstream of the tertiary diaphragm, is initially at partial vacuum (~ 10 's to

100's Pa), and is referred to as the 'acceleration tube'.

3. Test section and 'dump tank' (the right side of Fig. 1): the experiment occurs immediately downstream of the tube exit, and the remaining large volume of the dump tank is used to contain the gases that are generated during facility operation, ensuring that internal pressure remains sub-atmospheric upon completion of the experiment.

Upon its release, the piston accelerates to high speeds (typically 100-300 m/s⁵). The pressure of the 'driver' gas in front of the piston has only a minor impact on its trajectory until it has been compressed so much that the driver pressure rises from the fill condition to 10's MPa. At this point the piston transfers its significant kinetic energy into the driver gas, raising the driver gas temperature and pressure, and eventually rupturing the thick steel diaphragm. Following diaphragm rupture, shock tube flow is initiated; this corresponds to $t = 0$ in Fig. 1.

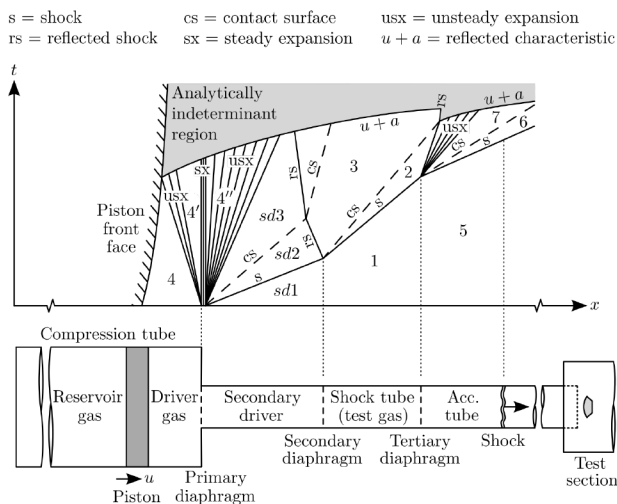


Fig. 1. Schematic diagram of wave processes in an expansion tube, commonly referred to as an $x-t$ diagram, taken from Gildfind et al.¹⁾

The key to the high performance of free-piston driven impulse facilities is the compressive heating of the driver gas, which enables the driver gas to be safely and efficiently processed from room temperature up to 1000's K, and 10's MPa pressure. The high temperature gas has a correspondingly high sound speed, and can therefore discharge its energy to the driven tube very rapidly. Combined with the high pressure of the driver gas, the free-piston driver can therefore drive stronger shocks than any reflected-shock facility. The piston compression process occurs over 10's to 100's ms, so

heat losses are acceptable, and thermal exposure to structural components occurs over such a short time that structural heating is likewise very limited.

Noting that $t = 0$ corresponds to the rupture of the primary diaphragm, Fig. 1 shows an *idealised* representation of the flow processes which arise following primary diaphragm rupture. The first section of the driven tube – the 'secondary driver' – is typically utilized for either of two reasons:

1. For high enthalpy conditions (~8-15 km/s), the secondary driver can be configured so that the sound speed of the shock-processed helium (Region $sd2$ in Fig. 1) is significantly higher than the sound speed of the expanded primary driver gas (Region $sd3$). Since the driven shock speed is so dependent on the sound speed of the driver gas, a secondary driver can therefore drive an even stronger shock in the test gas than the primary driver could by itself. While this operational method does not increase the available energy in the driver, it permits more rapid transfer of this energy, and this approach has proven necessary to achieve superorbital operation at the very limits of these machines⁶⁾.

2. For (relatively) low enthalpy conditions, such as scramjet flight between 3-5 km/s, it was previously found that significant noise in the primary driver gas (noise in Region $sd3$ produced by its expansion through the driver area change, and across the rupturing diaphragm) would transfer to the driven gas, and eventually manifest itself as unacceptable large amplitude noise in the test flow⁷⁾. Paull and Stalker⁷⁾ attributed this to the driven gas having a lower sound speed than the expanded driver gas, and suggested that the only way to avoid the transmission of this noise was to operate conditions where the shock-processed test gas had a higher sound speed, i.e. $a_{sd2} > a_{sd3}$, referred to as establishing an 'acoustic buffer'. If the primary driver is used to drive a shock directly into the test gas – i.e without the helium secondary driver depicted in Fig. 1 – then for low enthalpy conditions this acoustic buffer cannot be achieved. Morgan and Stalker⁶⁾ recognized that in such cases the acoustic buffer could be restored with a suitably configured secondary driver, and as such, this configuration is regularly used for scramjet test flows at UQ.

Referring to Fig. 1, the primary shock traverses the secondary driver and arrives at the secondary diaphragm. The diaphragm, which is only strong enough to contain the initial pressure difference between the two tubes, rapidly ruptures, and the shock

then proceeds to shock-process the test gas. If the test gas is sufficiently dense that the shock must slow down, a reflected shock forms, as shown in the figure; otherwise the Region *sd2* gas expands into the test gas, and the reflected shock in Fig. 1 is replaced with an expansion.

The shock-processed test gas (which may be air, or the gas from an alien atmosphere such as Mars or Titan) is compressed and accelerated towards the test section. Upon arrival at the third and final diaphragm, the tertiary diaphragm ruptures, and the test gas undergoes an unsteady expansion into the low pressure acceleration tube. The ‘expansion tube’ is named after this unsteady expansion process. Energy is transferred from the unexpanded upstream gas to the downstream expanded gas. Since the test gas is not stagnated during this process, these facilities are not subject to the stagnation pressure limits of other hypersonic facilities, such as RSTs. Only part of the test flow can be processed this way, so the test times are correspondingly short, however, no other facility can currently achieve the test flow stagnation properties of these facilities.

3. The UQ Expansion Tube Facilities

The University of Queensland currently operates two free-piston driven expansion tubes. X2, shown in Figs. 2 and 3, is a 23 m long facility, its driven tube has an 85mm diameter bore, and was originally commissioned in 1995⁸⁾. The facility is currently operated with a free-piston driver based on a lightweight 10.5 kg piston⁹⁾, a contoured Mach 10 nozzle (that can be removed), and is primarily used for studies of radiative heating during planetary entry (for example, the work of Eichmann²¹⁾), although it has also been used for scramjet testing (McGilvray¹⁰⁾) and proof-of-concept high Mach number scramjet flow condition development (Gildfind et al.¹¹⁾).

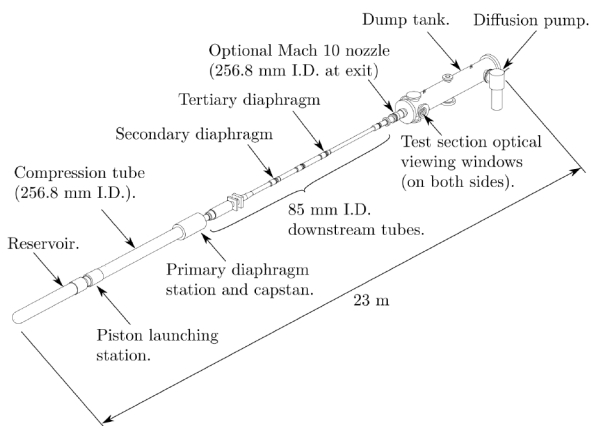


Fig. 2. Schematic diagram of X2 expansion tube facility, 2012 configuration, taken from Gildfind et al.¹¹⁾.

The X3 facility is much larger with a length of 62 m (considering both X2 and X3, these quoted lengths are nominal, and actual length will depend on the specific configuration of the specific test campaign), and a bore diameter of 182.6 mm through the driven sections. Originally commissioned in January 2001, X3 was originally operated with a dual piston driver, and was used successfully for several aerothermodynamic test campaigns targeting high enthalpy superorbital speeds¹⁰⁾. However, operational difficulties with the dual piston arrangement limited its performance and it was later upgraded to a high performance single piston free-piston driver¹⁰⁾. The new facility is currently operated with a 200 kg piston¹²⁾, and commissioning tests have also recently commenced with a lighter 101 kg piston¹³⁾.



Fig. 3. Photograph of X2; compression tube is shown in the foreground; acceleration tube and test section is shown in background.

In addition to the new driver, the facility upgrades also included a new contoured filament wound Mach 10 nozzle, manufactured from fiberglass¹⁴⁾, a new test section, new instrumentation, and various other upgrades¹²⁾. The upgraded facility is shown in Fig. 4, 5, and 6. At the time of writing a number of shots have been successfully performed with the new driver, nozzle, and test section. With its significant length this facility can achieve test times of between 100's μ s to 1 ms, will be able to test large models (the test flow core diameter is \sim 200 mm with the Mach 10 nozzle), and has world-class leading performance capabilities.



Fig. 4. X3's upgraded free-piston driver. Bore is \varnothing 500mm.

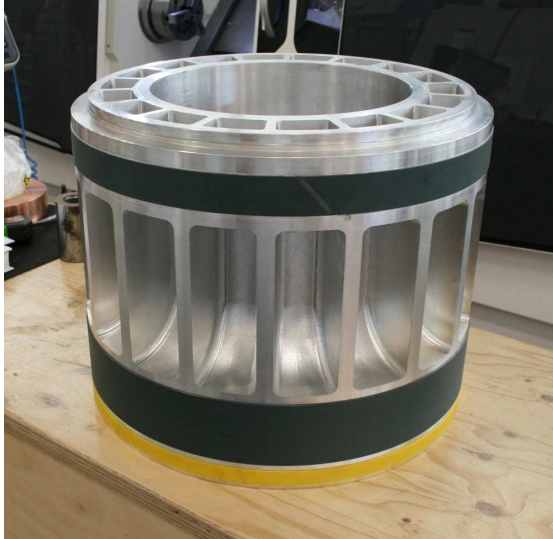


Fig. 5. X3's new 500 mm diameter lightweight piston, machined from 6061-T6 alloy, with total assembled mass of 100.8 kg¹³⁾.

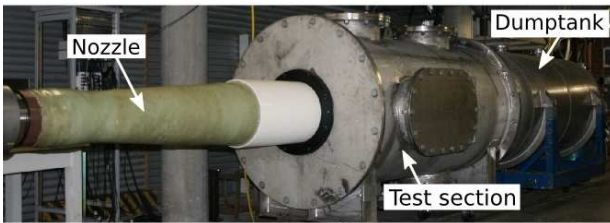


Fig. 6. X3's new fiberglass Mach 10 nozzle, test section, and dump tank.

4. Designing New Operating Conditions

The wave processes which arise in an expansion tube are complicated and difficult to control. However, the design of new flow conditions requires that the test gas is modeled appropriately, and that its actual properties can be accurately identified.

The assumed wave processes in the $x-t$ diagram shown in Fig 1. are largely based on the ideal gas analysis performed by Trimpi^{3,4)}, with modifications by subsequent authors for operation with a secondary driver (i.e. Morgan and Stalker⁶⁾). While these models have served as an essential reference for developing new conditions, specific *influential* wave processes for any given condition can be much more complicated.

Experience at UQ has found that the design of new flow conditions must be addressed differently depending on the flight enthalpy. For example, recent work with scramjet flow conditions, which are characterised by relatively 'slow' (by expansion tube standards) shock speeds through the test gas, has found that at low speeds there is close coupling of the wave

processes originating in the driver which cannot be ignored when developing new conditions¹⁾ (i.e. the transient development of each wave process over time does not necessarily occur independently of each other as is assumed multiple times in the idealised wave diagram shown in Fig. 1).

Fig. 7 shows an $x-t$ diagram computed by the 1-D Lagrangian code L1d⁶⁾, which can theoretically capture all of the longitudinal wave processes, including their interactions. The results are for a simulation of a (relatively) low enthalpy Mach 15 scramjet flow condition¹⁵⁾. The colors represent the log of static pressure, and experimental data points indicate close agreement with the computation for the primary shock wave. The diagram, which only captures 1-D wave processes, nevertheless demonstrates significantly greater complexity than Fig. 1, and wave interaction ('coupling') is also evident.

For higher enthalpy conditions, which form the focus of this present paper, critical wave processes transit the facility before upstream processes can have effect, and the wave model shown in Fig. 1 is more representative. However, higher enthalpy conditions have their own challenges, including:

1. High temperature gas effects. Ideal gas analyses over-predict the temperatures and can lead to invalid flow condition calculations at higher speeds.
2. Boundary layer or 'Mirels' effects^{17,18)}. Mass entrainment in the boundary layer behind a shock can lead to attenuation of a shock as it traverses a tube, resulting in slower observed shock speeds than those predicted by more idealised theory.
3. Effective nozzle area. The boundary layer that develops though a diverging contoured nozzle is flow condition dependent, and can significantly influence the degree of expansion of the test gas.

UQ has developed the sophisticated 2-D/3-D Navier-Stokes compressible flow solver, Eilmer3^{19, 23)}, which can model the physics of these hypersonic flow processes. However, these calculations require significant time and computational resources, and are not suitable for an iterative routine. UQ's 1-D code L1d, while capable of solving the facility response in a matter of hours, cannot account for 2-D processes which become important at these conditions.

Given these complexities, and to allow for the preliminary design and approximate characterization of new expansion tube test conditions within a reasonable time frame, it is important to have simple, approximate design tools which allow experimenters to design new test conditions quickly and easily, while incorporating sufficient flow physics to provide useful predictions.

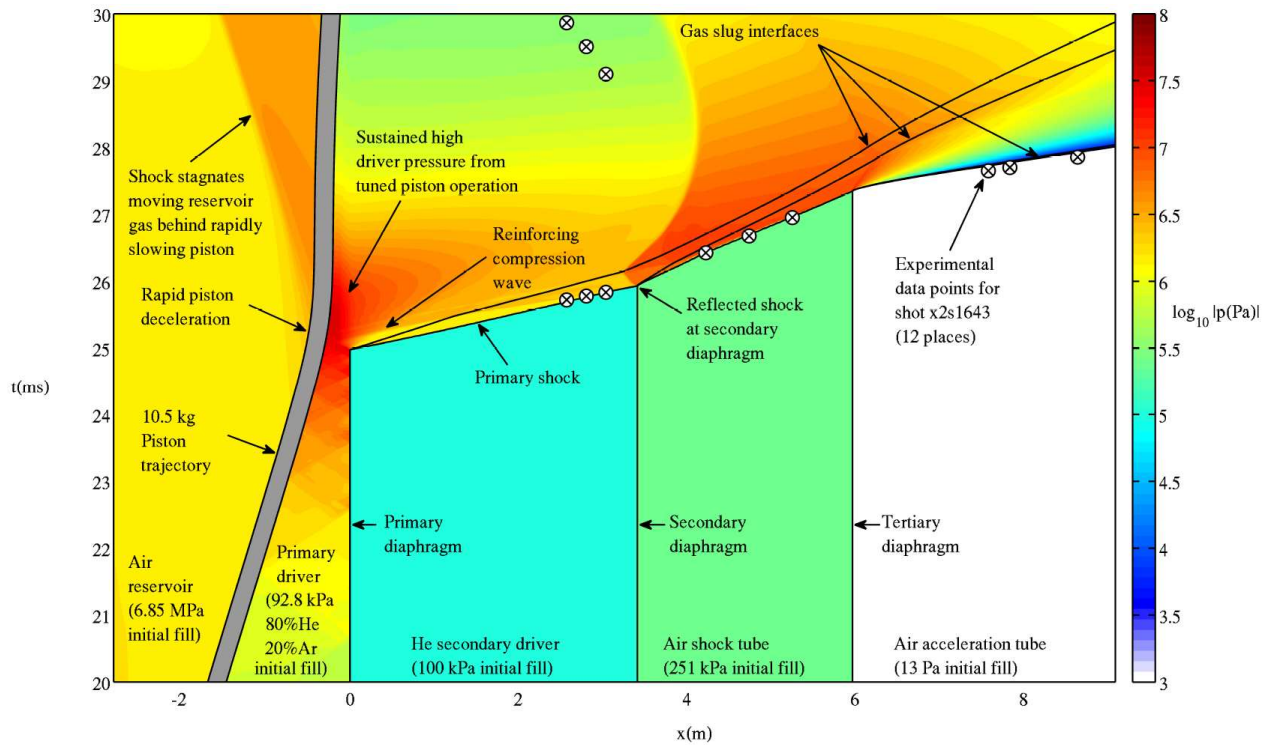


Fig. 7. $x-t$ diagram for Mach 15.0 flow condition, X2 without nozzle. Results are based on L1d2 calculations and experimental measurements¹⁵⁾.

In the following section a new code, PITOT, is described, and its performance is assessed against a series of actual flow conditions generated in UQ's X2 expansion tube.

5. The PITOT Code

5.1 Overview

PITOT is a simple Python-based expansion tube simulation code which was developed to act as a first 'port-of-call' tool for expansion tube condition design. Whereas 1-D and 2-D (axisymmetric) CFD codes respectively require, typically, tens and thousands of CPU hours to simulate the complex flow processes that occur in an expansion tube, PITOT can perform preliminary assessment of a flow conditions in the order of seconds, making it a potentially useful parametric design tool. This is possible because the PITOT code is based on an analytical model of the facility. In this respect, PITOT is no different to the traditional analytical codes which expansion tube experimenters have used over previous the decades that these machines have been in operation. However, where PITOT is different, is that it includes additional capabilities/flow physics which improve its flow condition estimates in comparison to codes based purely on the original ideal gas Trimpi analytical relations^{3,4)}. In addition, PITOT is structured to be a user-friendly, flexible, specialised expansion tube analysis tool, which *captures and proceduralises current best practice analysis techniques* for these machines, and fits within the wider hypersonics code

collection developed by UQ's Centre for Hypersonics²⁵⁾.

As noted previously, in the past, numerous experimenters, including those at UQ, have developed their own codes to make these types of calculations, normally made with perfect gas assumptions. Considering Fig.1, the perfect gas assumption is generally valid in both the secondary driver and shock tube, but for different reasons:

1. The secondary driver is filled with helium. As a monatomic gas, perfect gas relations remain accurate up to high shock speeds.
2. The shock tube, which can contain various test gases, *generally* has relatively low shock speeds (for example, 1.5-4 km/s), and therefore high temperature effects are less significant.

However, perfect gas assumptions can become problematic in the acceleration tube, normally filled with air, where for high enthalpy conditions, shock speeds can range between 8-15 km/s, resulting in very high post shock temperatures. At these high shock speeds, the temperature of the shock-processed accelerator gas is lower than that predicted by perfect gas models, and shock speeds are correspondingly overestimated through this acceleration tube.

PITOT is able to achieve more accurate predictions through the acceleration tube by incorporating an equilibrium gas model which accounts for high temperature effects. The code forms part of the CFCFD

code collection at The Centre for Hypersonics at The University of Queensland. The code takes advantage of existing, previously coded flow function in the group's code collection and interfaces with NASA's CEA program²⁴⁾ to capture high temperature effects.

These high temperature effects are illustrated in Fig. 8, for an 11 km/s Earth re-entry flow condition (using an air test gas, *without* a secondary driver). Experimental shock speeds are shown at different locations along the facility length; shock speed predictions based on 1) perfect gas assumptions, and 2) the PITOT code (labeled 'Equilibrium' in the plot) are also shown. Through the shock tube, experimental, equilibrium, and perfect gas results are observed to match closely. However, through the acceleration tube, the perfect gas solver overestimates the shock speed by 2000 m/s (~20%) compared to the PITOT code (equilibrium gas), which closely matches experimental results.

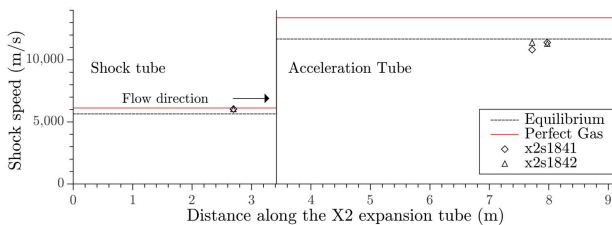


Fig. 8. Shock speed comparison between equilibrium and perfect gas solvers using a basic air condition. (100% He Primary Driver, 3 kPa Shock Tube, 10 Pa Acceleration Tube.)

PITOT was designed primarily to simulate the X2 and X3 expansion tubes, with and without the shock-heated secondary driver, and with and without a nozzle. However, it can also simulate a basic non-reflected shock tube, a configuration in which X2 is also occasionally operated. The following parameters are required:

- The primary driver fill pressure and composition.
- The primary diaphragm burst pressure.
- Knowledge of the area ratio between the driver and driven tubes, and any additional area contraction at this location (achieved through the use of orifice plates).

The ability to simulate Earth, Mars, Venus, Titan, and gas giant test gases are coded explicitly into PITOT for operator convenience, but the code also includes a custom test gas mode which allows the user to specify other test gases.

While PITOT is primarily intended as an equilibrium solver, it can be operated in two other modes:

1. It can be operated using perfect gas assumptions.
2. It can be operated in 'experiment' mode, whereby both experimental fill pressures *and* shock speeds are specified, and PITOT 'fills in the gaps' for the other parameters which cannot be measured.

5.1 PITOT Code Analytical Model

The main assumption that underpins the PITOT code is that an expansion tube can be simulated using simple isentropic flow relations. Comparisons between PITOT and experimental data for various *high* enthalpy flow conditions have shown that this assumption generally holds to a level that is satisfactory for a parametric design tool. However, for *lower* enthalpy scramjet conditions, as discussed previously, driver and driven wave processes become more complex and more coupled; in such cases the more computationally intensive 1-D L1d code may become necessary, even at the initial flow condition design stage.

This section details the way that PITOT simulates the expansion tube flow from start to finish.

1. Before a PITOT simulation is run, as with an actual experiment, the user must configure the 'virtual' facility by selecting a driver condition, selecting a test gas, specifying the fill pressure in the secondary driver (if used), and fill pressures in the shock tube (variable test gas) and the acceleration tube (air).
2. The compression of the driver gas from its initial fill condition up until the primary diaphragm bursts, is modeled as an isentropic compression up to the assumed primary diaphragm burst pressure. The driver gas at diaphragm burst is assumed to be stagnated ($M \sim 0$).
3. This hot, high pressure, stagnated driver gas is then steadily expanded to the appropriate Mach number which it will reach as it flows into the driven tube (the Mach number at the throat is calculated based on the area change at the primary driver, and the inclusion of any additional orifice plates/area contractions.)
4. The flows in the secondary driver (if used) and the shock tube are modeled in the same way. A property of a simple shock tube is that when a shock is being driven along the tube, an interface forms between the shocked driven gas (the gas being 'pushed'), and the expanded driver gas (the gas doing the 'pushing'), and across this interface, pressure and velocity are equal. PITOT uses an iterative secant-method solver to find the unique

combination of velocity and pressure at which both of these flow properties are equal across the interface. The code starts with a low shock speed in the secondary driver (or shock tube) and calculates the shock-processed properties of the shocked gas. The code then unsteadily expands the upstream driver gas up to this post-shock pressure. The corresponding velocities of the two gas regions are compared. The shock speed is then increased until the difference between the velocities of the driven and driver gases in the relevant section of the tube falls within a pre-defined maximum tolerance.

5. A similar process to step 4 is used to model the acceleration tube, but this process can be more complicated. As with step 4, a ‘first guess’ is made for the shock speed through the accelerator gas; the test gas is then unsteadily expanded to the pressure behind this shock. The velocity of the expanded test gas is then compared to the velocity of the shock-processed accelerator gas. If the velocity of the expanded test gas (Region 7 in Fig. 1) is higher than the velocity of the shock-processed accelerator gas (Region 6 in Fig. 1), then the assumed shock speed in the acceleration tube is increased. This process is repeated until velocities and pressures are *both* matched across the Region 6/7 interface. While this approach follows the basic methodology underpinning Fig. 1, the typically low density of the acceleration tube fill gas is such that the Mirels^{17,18)} effect can become too significant to ignore. As detailed in Section 4, the Mirels effect causes a further expansion of the test gas; in the limiting case, the test gas expands to the actual speed of the shock, and the Region 6/7 interface becomes stationary relative to the primary shock.

PITOT currently does not directly apply the methodology derived by Mirels^{17,18)} to account for this, but can instead *practically* account for the effect. It is common practice, when estimating test gas conditions, to assume the limiting case described above, and to expand the test gas to the *shock speed* in the acceleration tube (as opposed to the slightly lower shock-processed gas velocity provided by standard shock relations). PITOT offers this solution as a configuration option in the code; it is noted that the *actual* solution should theoretically lie between these two limits, and can be verified against experimental results.

6. UQ operates both its X2 and X3 facilities with Mach 10 contoured nozzles^{13,14)}. The Mach increase through these nozzles is theoretically based on the area ratio between the nozzle inlet and exit. However, the actual contour has been carefully designed to ensure that the exit flow is

parallel to the tunnel axis, and these optimised nozzle profiles are highly condition dependent. Both nozzles, which are designed for a Mach 10 exit flow, require a Mach 7.3 inflow^{13,14)}. However, even with this requirement met, boundary layer development for different flow conditions causes the *effective* area ratio of the nozzle to vary in between conditions.

If the expansion tube nozzle is included in PITOT, the nozzle expansion is modeled as a steady expansion through a *user specified* area ratio. The *geometric* area ratio of the nozzle is generally used as a starting point, but the nozzle expansion is a large potential source of inaccuracy, since the boundary layer development through the acceleration tube, and the nozzle itself, can result in an *effective* area ratio that is significantly different to the geometric area ratio.

To further improve nozzle modeling, PITOT includes a function that iterates through different area ratios, providing results at each ratio. These results can then be compared to experiment, allowing the most representative solution (i.e. the most representative effective area ratio) to be identified. However, there remains significant uncertainty in the computed result, and this calculation is much better handled by 2-D axisymmetric CFD (albeit at very high computational expense).

7. In addition, PITOT has options to apply the computed test flow to blunt models (by calculating the frozen and equilibrium conditions behind a normal shock) and 15° conehead models used for condition design (by calculating the conehead surface conditions using the Taylor-Maccoll equations).

5.2 Comparison Between Pitot and Experimental Data

For high enthalpy expansion tube conditions, PITOT has been observed to show good agreement with experiment. Fig. 8 shows that PITOT’s equilibrium solver predicts shock speeds well for a basic high enthalpy air condition. Figs. 9 and 10, reproduced from James et al²⁰⁾, show a comparison between PITOT, one dimensional equilibrium CFD performed using L1d¹⁶⁾, and experimental data; each plot shows a different simulated gas giant entry condition and test gases (H₂/He and H₂/Ne in Figs. 9 and 10 respectively). In Fig. 9 it can be seen that PITOT (the equilibrium solution) matches the three sets of experimental shock speeds well, and also the L1d simulation. In Fig. 10 it can be seen that PITOT (once again the equilibrium solution) matches the experimental shock speeds well, while the L1d simulation does not, which is attributed to an error

with that specific L1d gas model which is being addressed at the time of writing. James et al²⁰ also showed that for both test conditions, PITOT's approximation of the tube exit pressure was within the uncertainty range of the averaged experimental data.

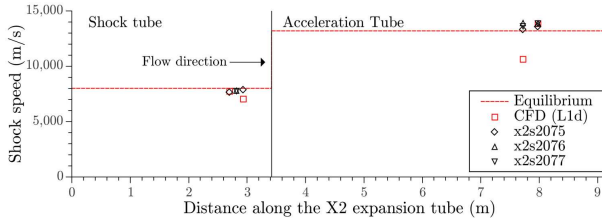


Fig. 9 Shock speed comparison for a H2/He gas giant entry condition between PITOT (equilibrium), experiment, and a 1-D CFD analysis performed using L1d from James et al²⁰.

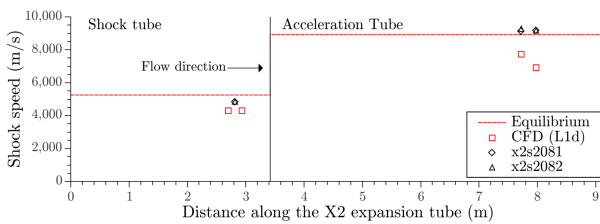


Fig. 10 Shock speed comparison for a H2/Ne gas giant entry condition between PITOT (equilibrium), experiment, and a 1-D CFD analysis performed using L1d from James et al²⁰.

5.3 Nozzle performance predictions

One of the key uncertainties in PITOT is the nozzle expansion, and as such, part of this study has investigated the use of CFD to solve the nozzle flow. It was hoped that applying a 2-D CFD calculation at the end of the PITOT analysis could provide a better estimation of flow properties at the nozzle exit with a reasonable increase in computational expense (compared to simulating the whole facility using transient 2-D CFD). However, performing a fully time resolved CFD analysis was deemed to be too time consuming, so a faster solver solving space-marching 2-D axisymmetric CFD code using an inflow from PITOT was chosen.

The T4 RST facility at UQ uses NENZFr (Non-Equilibrium Nozzle Flow reloaded) a space-marching version of Eilmer3²²) to characterise T4's nozzle outflow based on measured stagnation properties from the facility nozzle supply region. For an RST facility, where the nozzle flow expands from a stagnated condition with pressure that can be established experimentally, the initial conditions are, *in relative terms*, clearly defined. However, for an expansion tube operating at high enthalpies, where the inflow may be between 8 and 15 km/s, and where a complicated, and difficult to characterise, boundary layer will have already developed, defining appropriate

inflow conditions for the nozzle expansion is not so simple.

NENZFr was adapted to perform a 2D axisymmetric CFD analysis of a basic high enthalpy expansion tube air condition from X2 (the same condition used in Fig. 8). The inflow was radially uniform, with no boundary layer development, and non-equilibrium, equilibrium, and frozen simulations were conducted, using a fully turbulent inflow.

In Fig. 11 it can be seen that the initial results were promising, with a uniform Mach 10 outflow in the core flow for all three simulations. However, the same simulations failed to have a uniform pressure distribution over the same region, and a variation from 2.6 to 4kPa was observed in the core flow region (where the Mach number had been uniform).

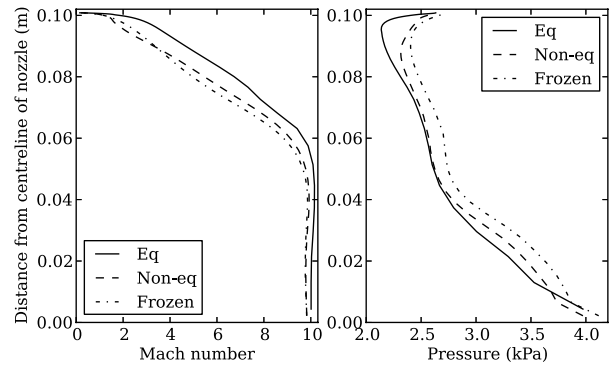


Fig. 11 Nozzle exit Mach number (left) and pressure (right) for three different NENZFr simulations of the same high enthalpy air condition in the X2 expansion tube.

Visualisation of the computed flow field showed that an oblique shock was forming at the edge of the nozzle inlet (the inflow boundary condition), which was causing local regions of low and high pressure throughout the nozzle, one of which was forming at the exit of the nozzle. To try and ascertain whether the absence of a straight section of tube leading into the nozzle was causing this issue (by producing an artificial disturbance), the original equilibrium simulation, which used a 0.0425 m lead in section (the NENZFr default is to use the value of the radius at the start of the nozzle as a lead in section) was recomputed using a 1m straight lead in section before the nozzle inlet. The result can be seen in Fig. 12. The longer straight section results in a more uniform computed exit pressure, but the nozzle exit Mach number is no longer uniform in the core flow.

Investigations are ongoing, however it is believed that the developed boundary layer must be included in the nozzle inflow for these 2-D nozzle calculations. Initial results reinforce the fact that flow through an expansion tube nozzle is complex, highly dependent on the

upstream flow processes which precede it, and is not easily modeled. It may be necessary to model the entire acceleration tube before the nozzle, in which case the computational expense may exceed that which can be tolerated for the intended application of the PITOT design tool. However, if a representative boundary layer profile can be estimated in PITOT, and better results can be obtained within a reasonable computation time (i.e. hours), this will provide an important additional capability for the PITOT code.

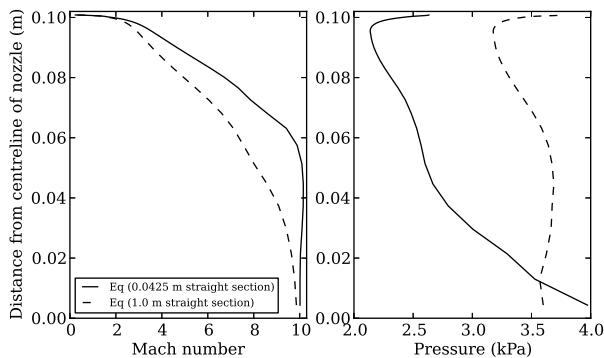


Fig. 12 Nozzle exit Mach number (left) and pressure (right) for two different equilibrium NENZFr simulations. The first simulation uses a 0.0425 m straight lead in section to the nozzle exit, while the second simulation uses 1 m lead in section.

7. Conclusions

This paper details a new expansion tube analysis code, PITOT. The code aims to provide a user-friendly, flexible, and specialised expansion tube analysis tool, which can be used to rapidly design new expansion tube flow conditions (i.e. to provide an effective ‘initial sizing’ tool for flow condition design), as well as rapidly characterise actual experimental test flows. PITOT does not aim to achieve the fidelity of 1-D and 2-D compressible flow codes, which remain essential for final characterization of test flows; rather, its aim is to provide a fast computation, making it suitable for parametric studies, and subject to this constraint, achieve maximum accuracy.

Furthermore, PITOT aims to capture best practice analysis techniques, and streamline their use on these facilities. The code fits within the wider hypersonics code collection developed by UQ’s Centre for Hypersonics. Compared to simpler analytical codes, PITOT robustly incorporates equilibrium gas effects to produce more accurate predictions of high enthalpy flow conditions. Ongoing work is also investigating ways to adapt the code to make usefully accurate nozzle flow calculations which can be performed much faster than the high fidelity, but computationally very expensive, calculations which are currently used.

Acknowledgments

The authors wish to thank Mr B. Loughrey, Mr F. De Beurs, and other members of the UQ Mechanical Engineering workshop, for continuing technical support for X2 and X3; the Australian Research Council for support and funding; The Queensland Smart State Research Facilities Fund 2005 for support and funding.

References

- 1) Gildfind, D.E., Morgan, R.G., McGilvray, M., Jacobs, P.A.: Production of High Mach Number Scramjet Flow Conditions in an Expansion Tube. Accepted for publication 7th Feb 2013 in AIAA Journal. In press.
- 2) Resler, E.L. and Bloxson, D.E.: Very High Mach Number Flows by Unsteady Flow Principles. Cornell University Graduate School of Aeronautical Engineering, Limited Distribution Monograph, January 1952.
- 3) R.L. Trimpi: A preliminary theoretical study of the expansion tube, a new device for producing high-enthalpy short-duration hypersonic gas flows, NASA Technical Report R-133, NASA Langley Research Centre, Langley Station, Hampton, Va (1962).
- 4) R.L. Trimpi: A theoretical Investigation of Simulation in Expansion Tubes and Tunnels, NASA TR R-243, NASA Langley Research Centre, Langley Station, Hampton, Va (1966).
- 5) R. Morgan. Handbook of Shock Waves, Volume 1, chapter 4.2 Free Piston Driven Reflected Shock Tunnels, pages 587–601. Academic Pres, 2001.
- 6) R.G. Morgan and R.J. Stalker. Double Diaphragm Driven Free Piston Expansion Tube. In 18th International Symposium on Shock Waves, Jul 21-26, Sendai, Japan, 1991.
- 7) A. Paull and R.J. Stalker. Test flow disturbances in an expansion tube. Journal of Fluid Mechanics, **245**:493–521, 1992.
- 8) Scott, M. P., Development and Modelling of Expansion Tubes, Ph.D. thesis, Centre for Hypersonics, Department of Mechanical Engineering, University of Queensland, 2006.
- 9) D.E. Gildfind, R.G. Morgan, M. McGilvray, P.A. Jacobs, R.J. Stalker, and T.N. Eichmann. Free-Piston Driver Optimisation for Simulation of High Mach Number Scramjet Flow Conditions. Shock Waves, 21:6, pp 559-572, 2011.
- 10) M. McGilvray. The use of expansion tube facilities for scramjet testing. PhD thesis, Centre for Hypersonics, Department of Mechanical Engineering, University of Queensland, Jan 2008.
- 11) Gildfind, D.E., Jacobs, P.A., Morgan, R.G.: Vibration Isolation in a Free-Piston Driven Expansion Tube Facility. Shock Waves, **23**:5, pp 431-438, 2013.
- 12) Dann, A.G., Morgan, R.G., Gildfind, D.E., Jacobs, P.A., McGilvray, M., and Zander, F.: Upgrade of the X3 Super-orbital Expansion Tube, 18th Australasian Fluid Mechanics Conference, Launceston, Australia, 3-7 December 2012.
- 13) Gildfind, D.E., Morgan, R.G., Sancho, J., Design and Commissioning of a New Lightweight Piston for the X3 Expansion Tube. The 29th International Symposium on Shock Waves, Madison, Wisconsin, USA, 14–19 July 2013.
- 14) Michael G. Davey. A Hypersonic Nozzle for the X3 Expansion Tube. Bachelor of Engineering Thesis, Department of Mechanical Engineering, University of Queensland, 2006.
- 15) Gildfind, D., Development of High Total Pressure Scramjet Flow Conditions using the X2 Expansion Tube, Ph.D. thesis, Division of Mechanical Engineering, School of Engineering,

- The University of Queensland, Brisbane, Australia, 2012.
- 16) Peter A. Jacobs. Shock Tube Modelling with L1d. Research Report 13/98, Department of Mechanical Engineering, The University of Queensland, Nov 1998.
 - 17) H. Mirels. Test Time in Low-Pressure Shock Tubes. *The Physics of Fluids*, 6(9):1201–1214, 1963.
 - 18) H. Mirels. Shock Tube Test Time Limitation Due to Turbulent-Wall Boundary Layer. *AIAA Journal*, 2(1):84–93, 1963.
 - 19) Jacobs, P. and Gollan, R., The Eilmer3 Code: User Guide and Example Book. Mechanical Engineering Report 2008/07, University of Queensland, 2009.
 - 20) C.M James, D.E. Gildfind, R.G. Morgan, T.J. McIntyre. Working Towards Simulating Gas Giant Entry Radiation in an Expansion Tube. The 29th International Symposium on Shock Waves, Madison, Wisconsin, USA, 14–19 July 2013.
 - 21) Eichmann, T., Radiation Measurements in a Simulated Mars Atmosphere, Ph.D. thesis, the University of Queensland, St. Lucia, Australia, 2012.
 - 22) Jacobs, P.A. and Gollan, R.J. and Zander, F., Still Using NENZF? That’s so 1960’s, 11th International Workshop on Shock Tube Technology, Brisbane, Australia, 21-25 March 2011.
 - 23) Gollan, R. J. and Jacobs, P. A., About the formulation, verification and validation of the hypersonic flow solver Eilmer. *International Journal for Numerical Methods in Fluids*, 73:1, pp19-57, 2013.
 - 24) McBride, D. and Gordon, G., Computer Program for Calculations of Complex Chemical Equilibrium Compositions and Applications II. Users Manual and Program Description, Nasa Lewis Research Center, Cleveland, OH, U.S.A, 1996.
 - 25) Jacobs, P. and Gollan, R., “The Compressible-Flow CFD Project,” <http://www.mech.uq.edu.au/cfcfd/>, Dec. 2012, Accessed December 21, 2012.